SUPPORTING INFORMATION

The effect of the disposition of coordinated oxygen atoms on the magnitude of the energy barrier for magnetization reversal in a family of linear trinuclear Zn-Dy-Zn complexes with square-antiprism DyO_8 coordination sphere

Itziar Oyarzabal, Antonio Rodríguez-Diéguez, Montserrat Barquin, José M. Seco and Enrique Colacio

Table S.1.- Crystallographic data for complexes **1-6**.

Complex	**1**	**2**	**3**	**4**	**5**	**6**
Formula	$C_{41}H_{44}N_5O_{12}Cl_2Br_4Zn_2Dy$	$C_{42}H_{52}N_4O_{12}Br_9Zn_3Dy$	$C_{43}H_{52}N_5O_{14}Br_6Zn_2Dy$	$C_{41}H_{44}N_4O_{12}Br_4I_3Zn_2Dy$	$C_{43}H_{52}N_5O_{14}Br_4I_2Zn_2Dy$	$C_{41}H_{46}N_{11}O_{13}Br_4Zn_2Dy$
M_r	1482.59	1882.67	1635.59	1778.38	1729.57	1513.77
Crystal system	Triclinic	Monoclinic	Monoclinic	Monoclinic	Monoclinic	Triclinic
Space group (no.)	*P-1* (2)	*P21/n* (14)	*P21/c* (14)	*P21/c* (14)	*P21/c* (14)	*P-1* (2)
a (Å)	11.820(2)	14.6756(11)	14.6274(3)	14.9193(3)	14.7655(3)	13.6069(7)
b (Å)	12.875(2)	13.0146(9)	27.3664(5)	25.4989(3)	27.0577(4)	13.8358(9)
c (Å)	15.948(3)	30.607(2)	14.7306(4)	15.6761(3)	15.1740(3)	15.9283(7)
a (°)	98.179(3)	90	90	90	90	99.998(5)
β (°)	94.615(3)	93.627(2)	115.170(3)	116.881(2)	115.552(2)	108.143(5)
γ (°)	91.774(3)	90	90	90	90	106.028(5)
V ($Å^3$)	2392.2(7)	5834.1(7)	5336.8(2)	5319.21(18)	5469.39(19)	2625.9(3)
Z	2	4	4	4	4	2
D_c (g cm^{-3})	2.058	2.143	2.036	2.221	2.100	1.851
m(MoK_a) (mm^{-1})	6.058	8.705	6.836	7.090	6.338	5.421
*T (*K)	100(2)	100(2)	100(2)	100(2)	100(2)	100(2)
Observed reflections	10772 (9031)	14924 (12409)	11840 (8854)	12209 (10629)	12541 (10581)	11643 (7756)
R_{int}	0.0442	0.0664	0.0564	0.0325	0.0331	0.0610
Parameters	610	647	650	609	627	590
GOF	1.009	1.065	1.026	1.053	1.051	0.951
R_1[a,b]	0.0444 (0.0352)	0.0698 (0.0551)	0.0811 (0.0533)	0.0545 (0.0460)	0.0558 (0.0441)	0.0959 (0.0587)
wR_2[c]	0.0832 (0.0785)	0.1357 (0.1254)	0.1235 (0.1085)	0.1225 (0.1177)	0.1083 (0.1022)	0.1254 (0.1114)
Largest difference in peak and hole (e $Å^{-3}$)	1.599 and -0.735	3.740 and -3.322	2.139 and -2.347	2.041 and -4.678	5.120 and -1.786	1.858 and -1.692

[a] $R_1 = S||F_o| - |F_c||/S|F_o|$. [b] Values in parentheses for reflections with $I > 2s(I)$. [c] $wR_2 = \{S[w(F_o^2 - F_c^2)^2] / S[w(F_o^2)^2]\}^{½}$

Table S.2.- Selected bond lengths (Å) and angles (°) for complexes **1-6**.

Complex	**1**	**2**	**3**	**4**	**5**	**6**
Dy(1)···Zn(1)	3.553(1)	3.573(1)	3.569(1)	3.568(1)	3.571(1)	3.568(1)
Dy(1)···Zn(2)	3.534(1)	3.572(1)	3.562(1)	3.546(1)	3.564(1)	3.591(1)
Dy(1)-O(1A)	2.385(3)	2.393(4)	2.385(4)	2.378(5)	2.389(5)	2.364(5)
Dy(1)-O(2A)	2.290(3)	2.335(4)	2.321(5)	2.329(5)	2.243(4)	2.350(5)
Dy(1)-O(3A)	2.321(3)	2.235(4)	2.239(4)	2.246(5)	2.333(4)	2.263(4)
Dy(1)-O(4A)	2.392(3)	2.448(4)	2.393(5)	2.414(5)	2.390(4)	2.454(5)
Dy(1)-O(1B)	2.388(3)	2.405(4)	2.408(5)	2.387(5)	2.403(4)	2.397(5)
Dy(1)-O(2B)	2.303(3)	2.330(4)	2.277(5)	2.322(5)	2.310(4)	2.340(4)
Dy(1)-O(3B)	2.317(3)	2.251(4)	2.316(5)	2.264(5)	2.279(4)	2.261(5)
Dy(1)-O(4B)	2.374(3)	2.426(4)	2.401(4)	2.416(5)	2.405(5)	2.412(5)
Zn(1)-N(1A)	2.123(3)	2.173(5)	2.151(6)	2.169(6)	2.141(5)	2.133(6)
Zn(1)-N(2A)	2.145(3)	2.102(5)	2.145(6)	2.124(6)	2.158(5)	2.111(6)
Zn(1)-O(2A)	2.137(3)	2.055(4)	2.081(4)	2.098(5)	2.101(4)	2.044(5)
Zn(1)-O(3A)	2.066(3)	2.148(4)	2.078(5)	2.100(5)	2.078(4)	2.125(5)
Zn(1)-X(1A)	2.214(1)	2.356(1)	2.360(1)	2.556(1)	2.5421(8)	1.992(6)

Table S.2.- Continuation.

Complex	**1**	**2**	**3**	**4**	**5**	**6**
Zn(2)-N(1B)	2.138(4)	2.163(5)	2.098(5)	2.182(6)	2.188(5)	2.154(6)
Zn(2)-N(2B)	2.153(4)	2.122(5)	2.186(6)	2.115(6)	2.105(5)	2.114(6)
Zn(2)-O(2B)	2.087(3)	2.057(4)	2.166(5)	2.058(5)	2.043(4)	2.058(4)
Zn(2)-O(3B)	2.101(3)	2.142(4)	2.047(5)	2.156(5)	2.171(4)	2.147(5)
Zn(2)-X(1B)	2.218(1)	2.355(1)	2.372(1)	2.570(1)	2.559(1)	1.971(7)
Zn(3)-Br(1C)		2.378(2)				
Zn(3)-Br(2C)		2.385(2)				
Zn(3)-Br(3C)		2.350(2)				
Zn(3)-O(4M)		2.009(8)				
Dy(1)-O(2A)-Zn(1)	106.73(11)	108.82(17)	108.23(19)	107.29(19)	110.55(17)	108.4(2)
Dy(1)-O(3A)-Zn(1)	108.08(11)	109.20(17)	111.5(2)	110.3(2)	107.97(17)	108.8(2)
Dy(1)-O(2B)-Zn(2)	107.16(11)	108.87(17)	106.59(19)	107.99(19)	109.73(18)	109.3(2)
Dy(1)-O(3B)-Zn(2)	106.18(11)	108.79(17)	109.3(2)	106.68(19)	106.38(17)	109.1(2)
O(2A)-Zn(1)-O(3A)	75.96(10)	74.23(15)	73.79(18)	74.62(18)	74.29(15)	75.56(18)
O(2B)-Zn(2)-O(3B)	76.47(10)	74.30(15)	75.46(18)	75.69(18)	75.23(16)	74.25(18)
O(2A)-Dy(1)-O(3A)	68.26(9)	67.41(14)	66.36(16)	67.55(17)	66.91(14)	67.24(16)
O(2B)-Dy(1)-O(3B)	68.28(9)	67.22(14)	68.32(16)	68.66(16)	68.24(14)	66.97(17)
Zn(1)-Dy(1)-Zn(2)	105.94(2)	143.743(17)	146.77(2)	146.95(2)	146.249(18)	141.56(2)

Table S.3.- Shape measures for Dy(III) coordination environments in complexes **1-6**.

Complex	SAPR-8	TDD-8	JBTPR-8	BTPR-8	JSD-8
1	0.504	2.590	3.078	2.405	5.492
2	0.804	2.329	3.435	2.982	5.837
3	0.544	2.367	2.974	2.454	5.296
4	0.458	2.227	2.892	2.454	5.317
5	0.510	2.377	2.957	2.450	5.384
6	1.060	2.160	3.574	3.142	5.868

* SAPR-8: square antiprism (D_{4d}); TDD-8: triangular dodecahedron (D_{2d}); JBTPR-8: Biaugmented trigonal prism J50 (C_{2v}); BTPR-8: biaugmented trigonal prism (C_{2v}); JSD-8: Snub diphenoid J84 (D_{2d}).

*Shape measures relative to other reference polyhedron are significantly larger.

Table S.4- Shape measures for Zn(II) coordination environments in complexes **1-6**.

Complex	PP-5	vOC-5	TBPY-5	SPY-5	JTBPY-5
1-Zn1	32.663	3.344	4.331	0.572	7.493
1-Zn2	32.571	3.700	4.595	0.687	8.146
2-Zn1	33.426	4.677	3.833	1.223	7.206
2-Zn2	33.651	4.559	4.166	1.118	7.675
3-Zn1	32.887	4.792	4.126	1.242	8.049
3-Zn2	33.765	4.569	4.677	1.017	8.041
4-Zn1	33.807	5.574	4.321	1.714	8.478
4-Zn2	33.941	5.627	4.732	1.662	8.603
5-Zn1	34.333	5.532	4.383	1.650	8.560
5-Zn2	34.123	5.478	5.135	1.504	8.914
6-Zn1	31.976	2.884	3.369	0.696	5.913
6-Zn2	31.454	2.979	3.609	0.730	6.058

*PP-5: pentagon (D_{5h}); vOC-5: vacant octahedron (C_{4v}); TBPY-5: trigonal bipyramid (D_{3h}); SPY-5: square pyramid (C_{4v}); JTBPY-5: Johnson trigonal bipyramid (D_{3h}).

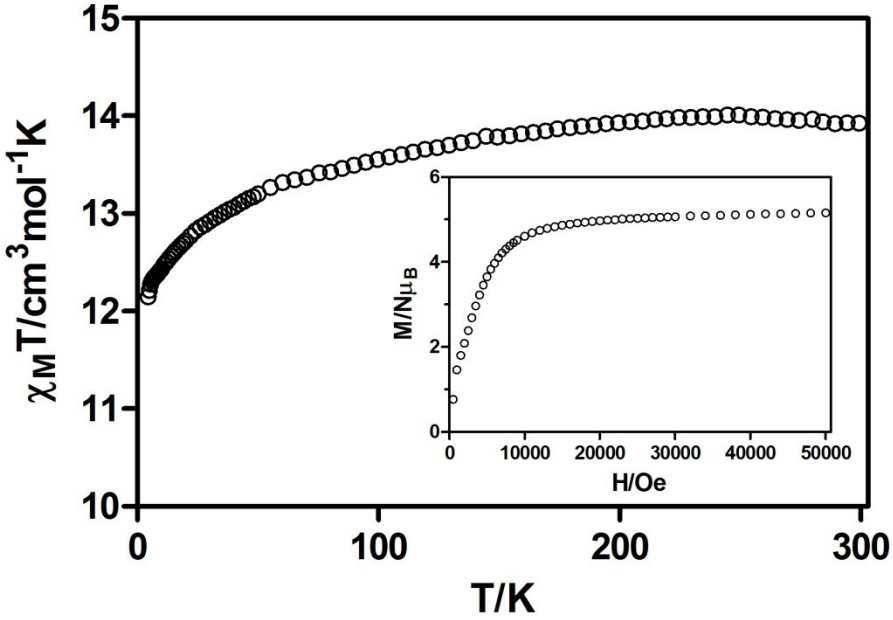

Figure S.1.- Temperature dependence of $\chi_M T$ for **1**. Inset: Field dependence of the molar magnetization for **1**.

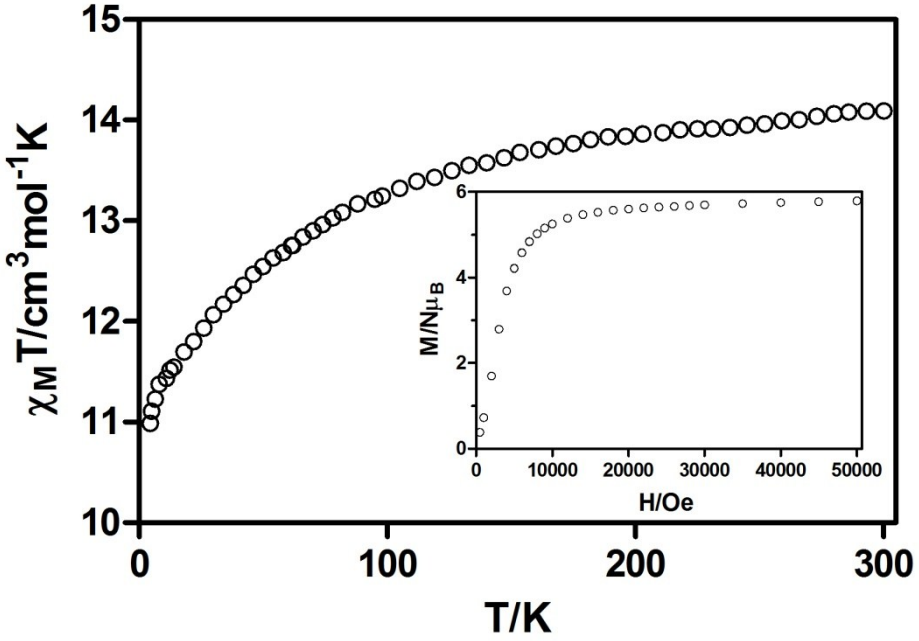

Figure S.2.- Temperature dependence of $\chi_M T$ for **2**. Inset: Field dependence of the molar magnetization for **2**.

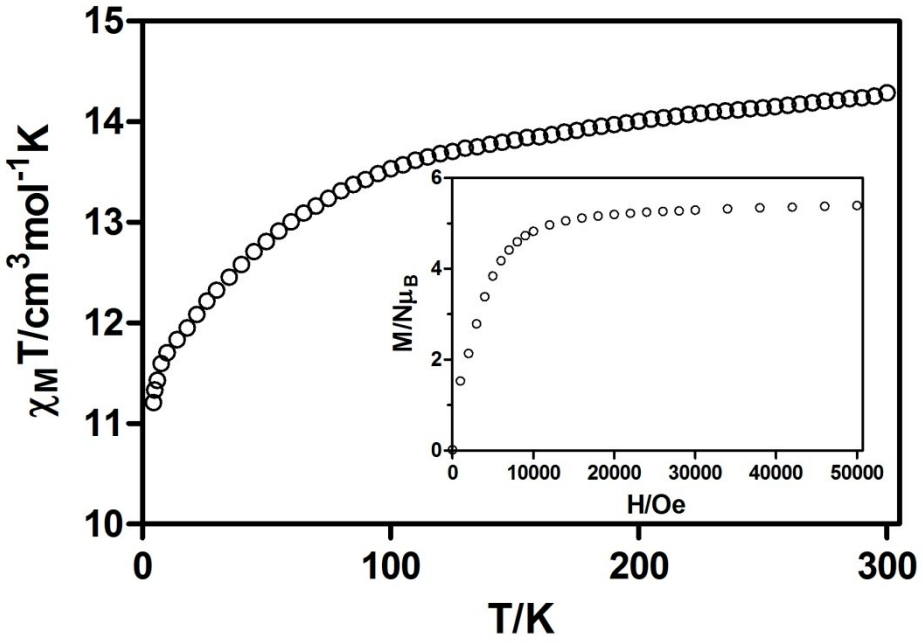

Figure S.3.- Temperature dependence of $\chi_M T$ for **3**. Inset: Field dependence of the molar magnetization for **3**.

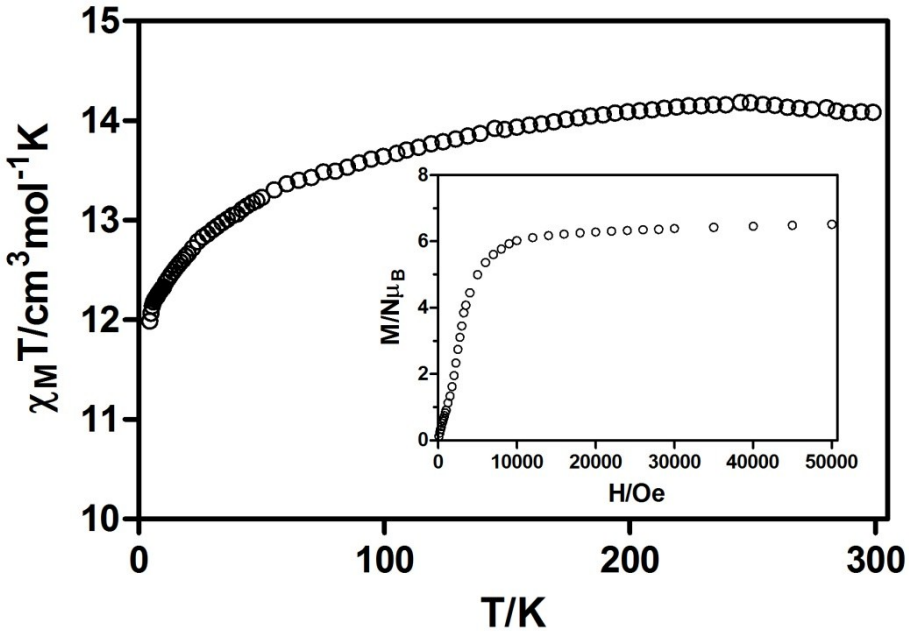

Figure S.4.- Temperature dependence of $\chi_M T$ for **4**. Inset: Field dependence of the molar magnetization for **4**.

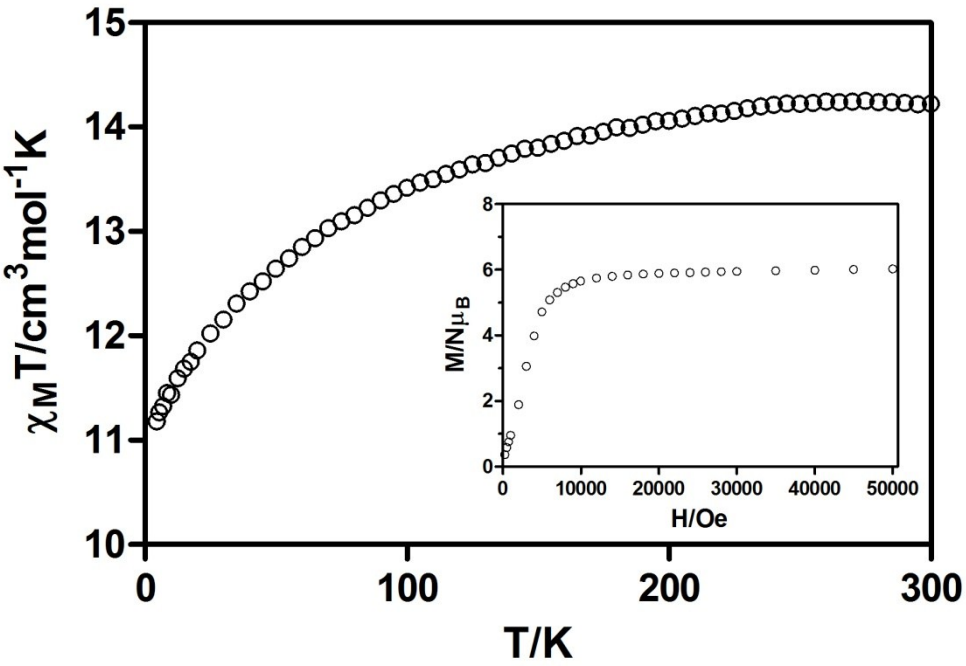

Figure S.5.- Temperature dependence of $\chi_M T$ for **5**. Inset: Field dependence of the molar magnetization for **5**.

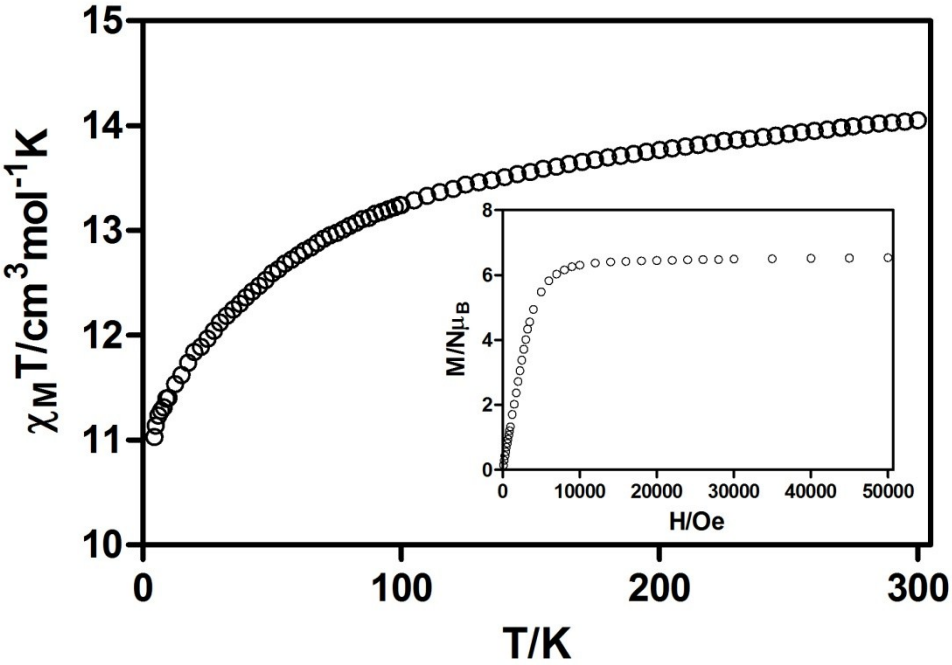

Figure S.6.- Temperature dependence of $\chi_M T$ for **6**. Inset: Field dependence of the molar magnetization for **6**.

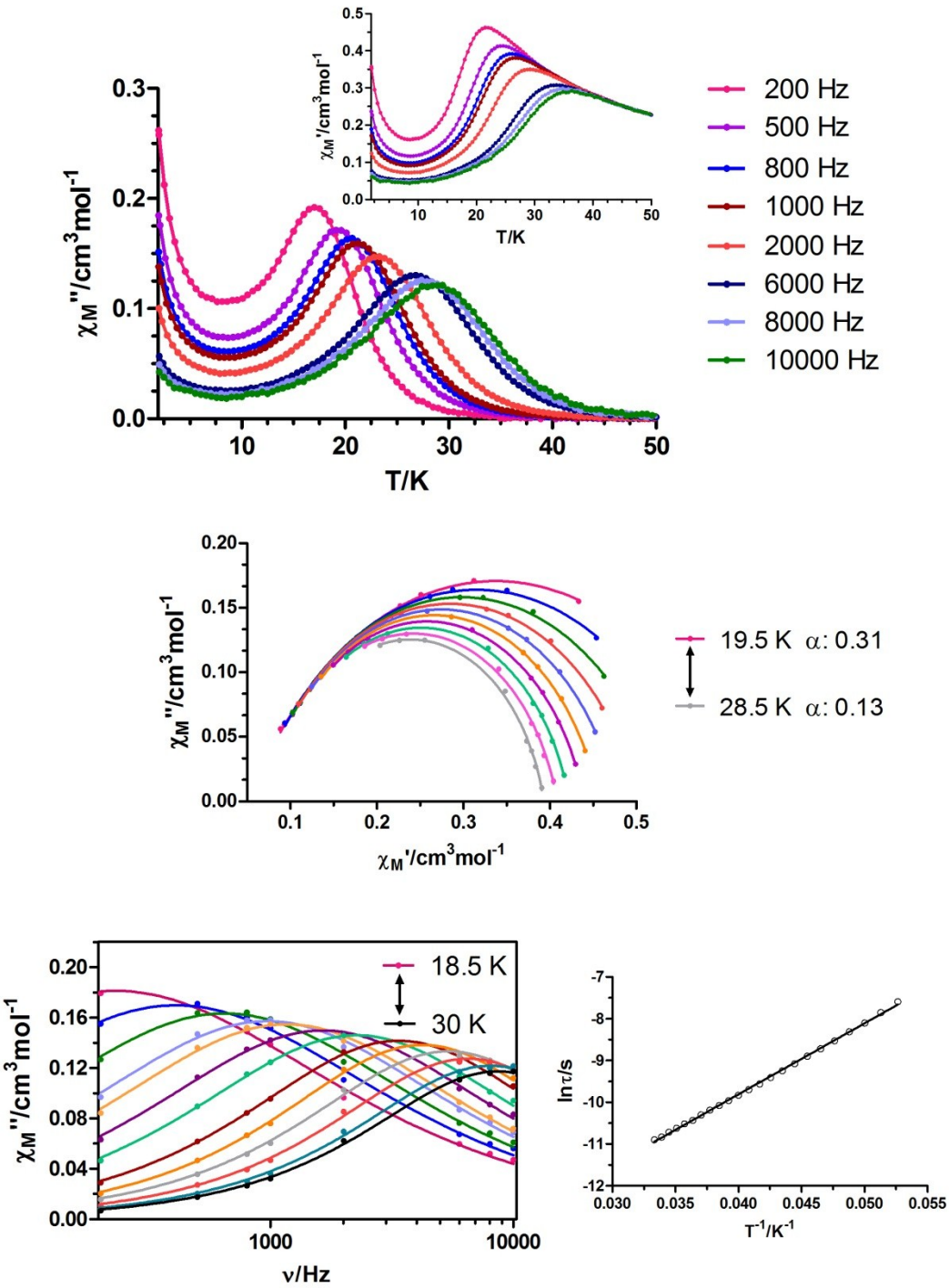

Figure S.7.- Top: temperature dependence of in-phase χ_M' (inset) and out-of phase χ_M'' components of the *alternating current* susceptibility for complex **1** under zero applied external field. Medium: Cole-Cole plot. Bottom left: variable-temperature frequency dependence of the χ_M'' signal. Bottom right: Arrhenius plots for the relaxation of **1** (black line).

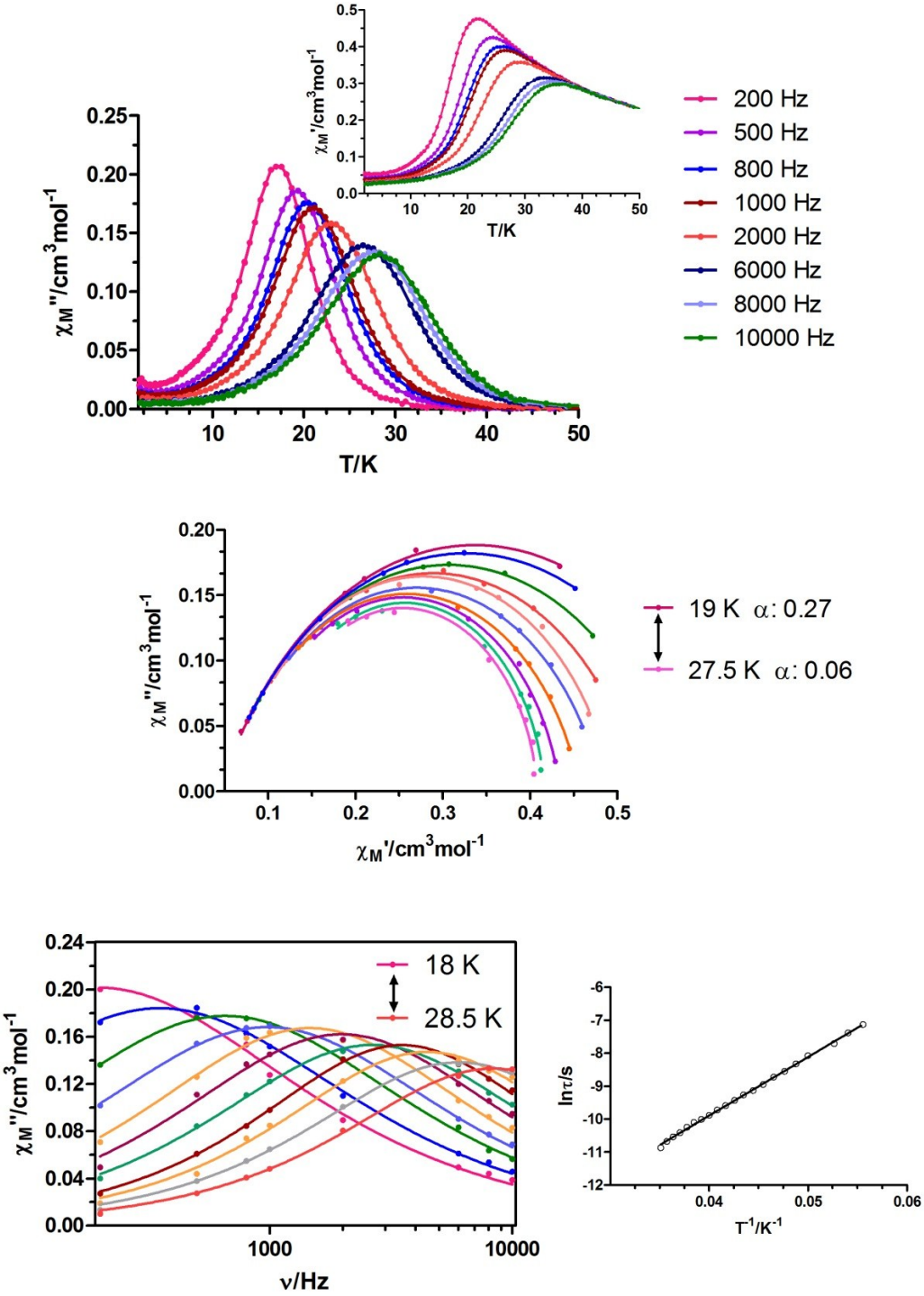

Figure S.8.- Top: temperature dependence of in-phase χ_M' (inset) and out-of phase χ_M'' components of the *alternating current* susceptibility for complex **1** under 1000 Oe applied external field. Medium: Cole-Cole plot. Bottom left: variable-temperature frequency dependence of the χ_M'' signal. Bottom right: Arrhenius plots for the relaxation of **1** (black line).

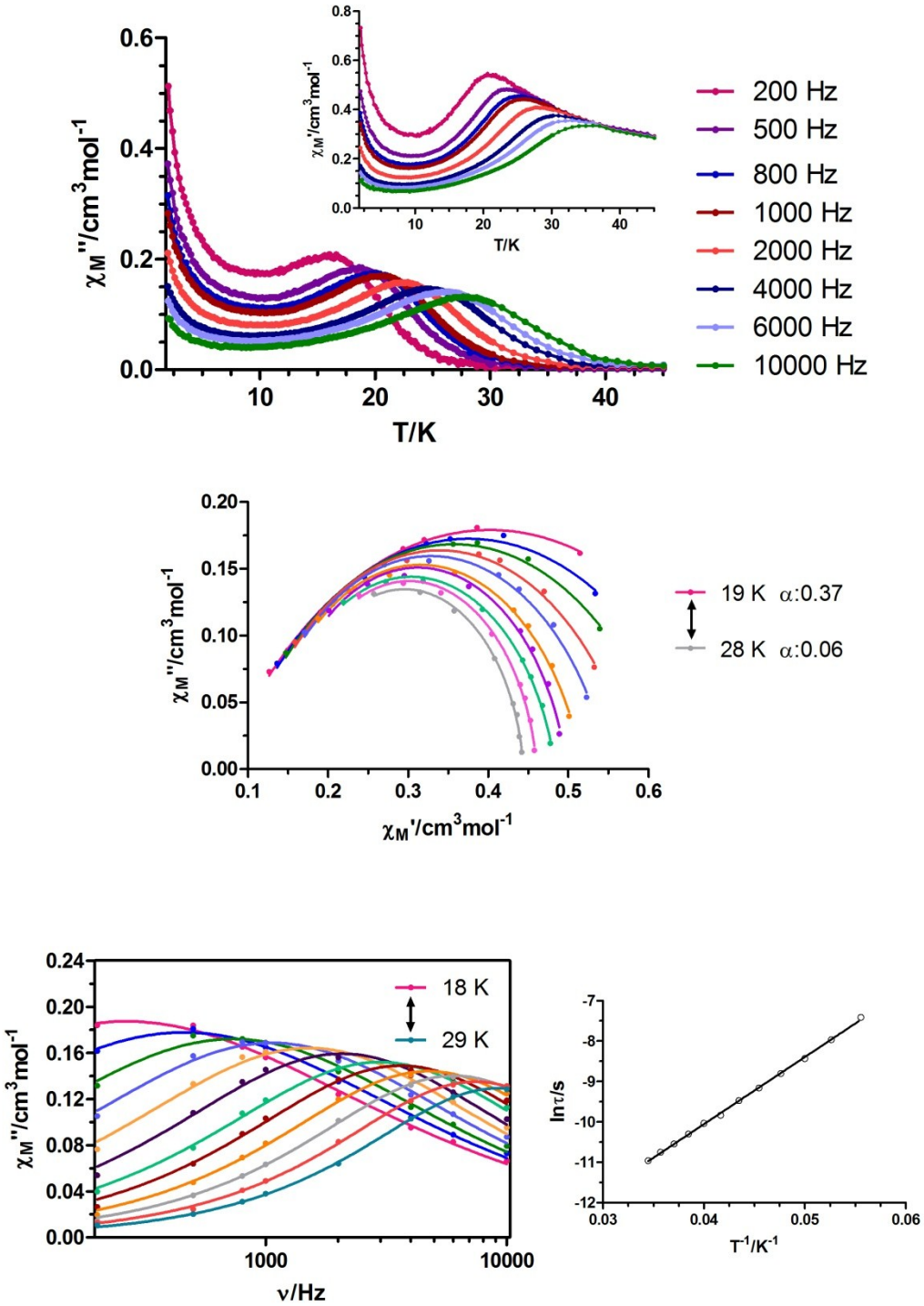

Figure S.9.- Top: temperature dependence of in-phase χ_M' (inset) and out-of phase χ_M'' components of the *alternating current* susceptibility for complex **2** under zero applied external field. Medium: Cole-Cole plot. Bottom left: variable-temperature frequency dependence of the χ_M'' signal. Bottom right: Arrhenius plots for the relaxation of **2** (black line).

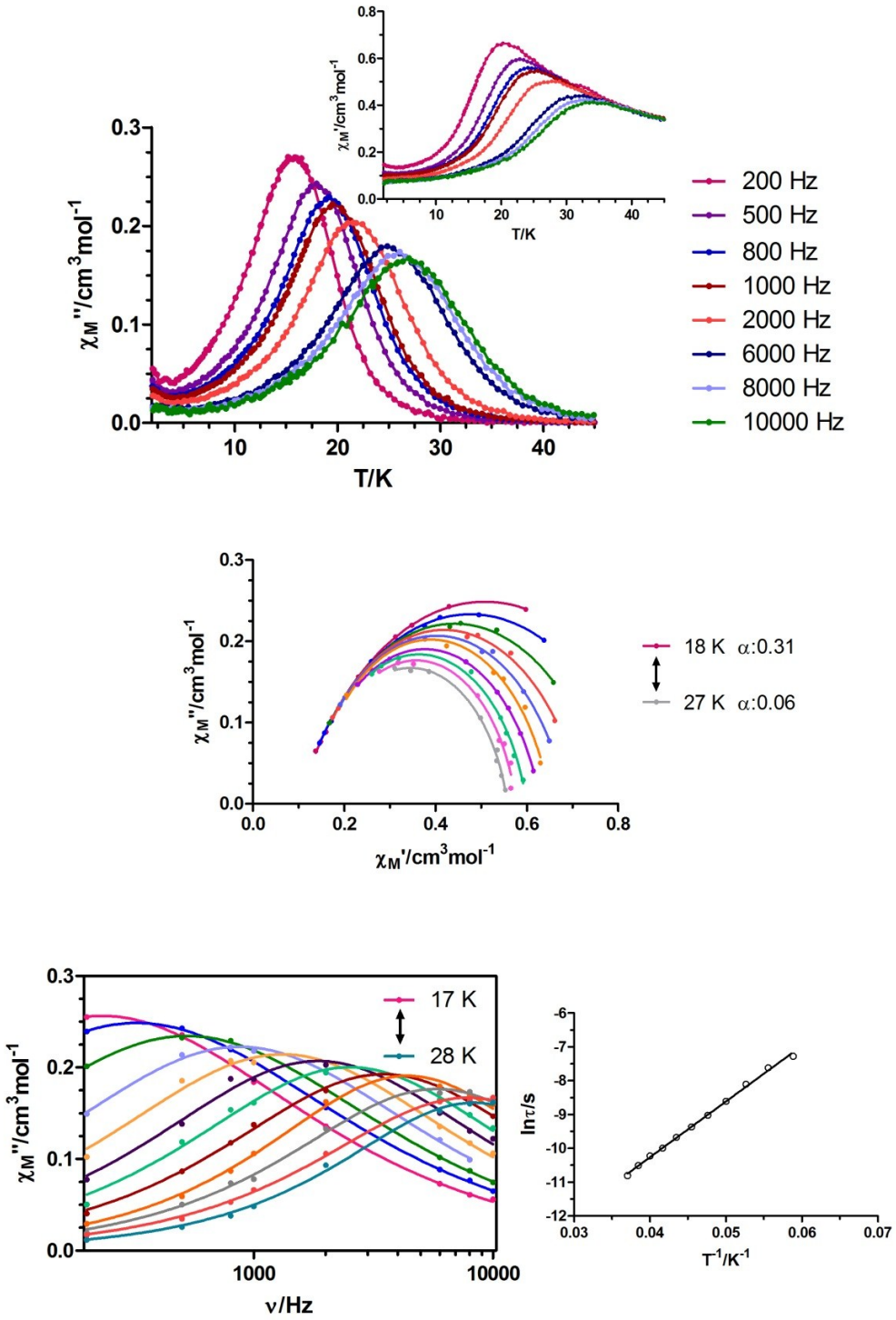

Figure S.10.- Top: temperature dependence of in-phase χ_M' (inset) and out-of phase χ_M'' components of the *alternating current* susceptibility for complex **2** under 1000 Oe applied external field. Medium: Cole-Cole plot. Bottom left: variable-temperature frequency dependence of the χ_M'' signal. Bottom right: Arrhenius plots for the relaxation of **2** (black line).

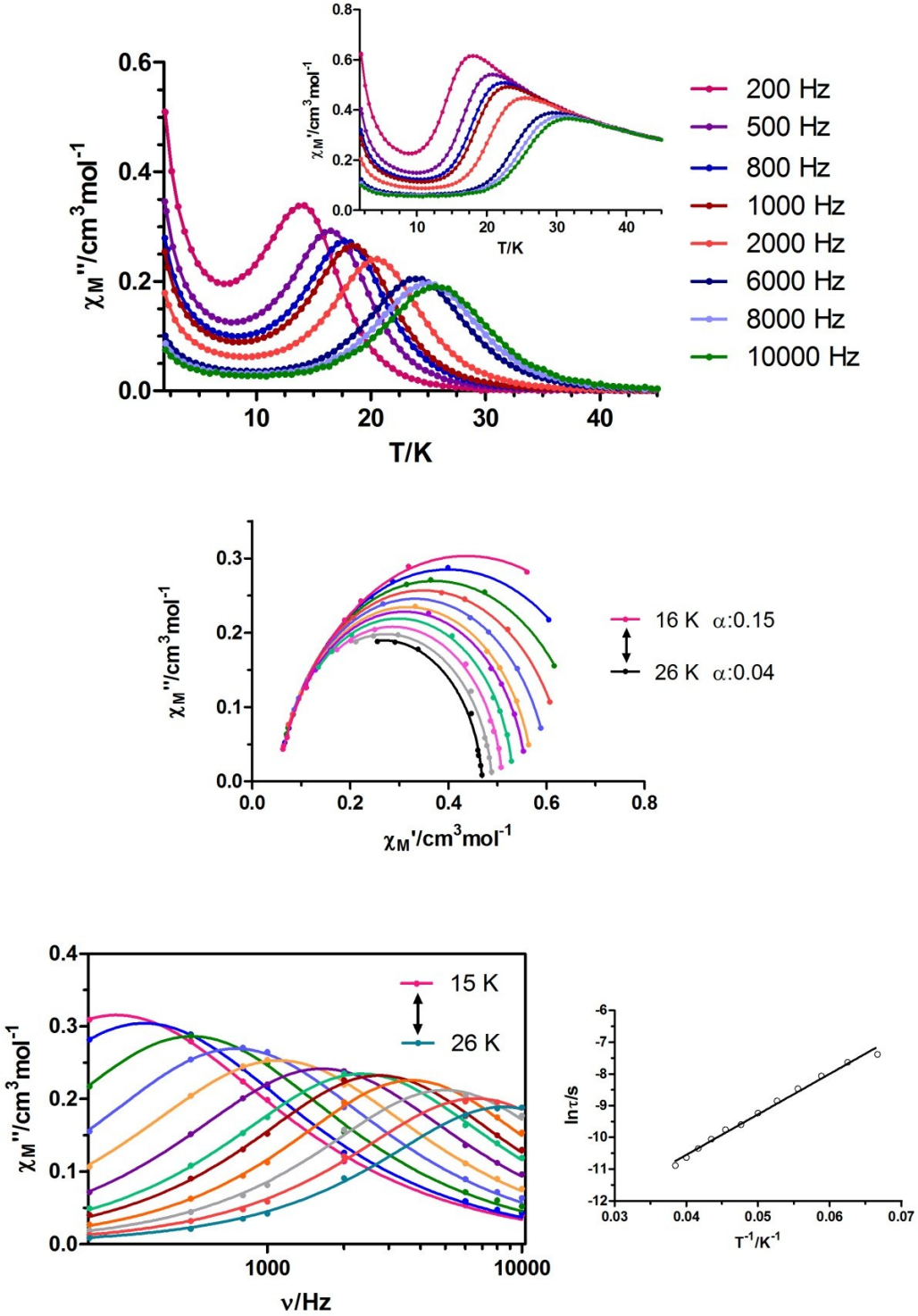

Figure S.11.- Top: temperature dependence of in-phase χ_M' (inset) and out-of phase χ_M'' components of the *alternating current* susceptibility for complex **3** under zero applied external field. Medium: Cole-Cole plot. Bottom left: variable-temperature frequency dependence of the χ_M'' signal. Bottom right: Arrhenius plots for the relaxation of **3** (black line).

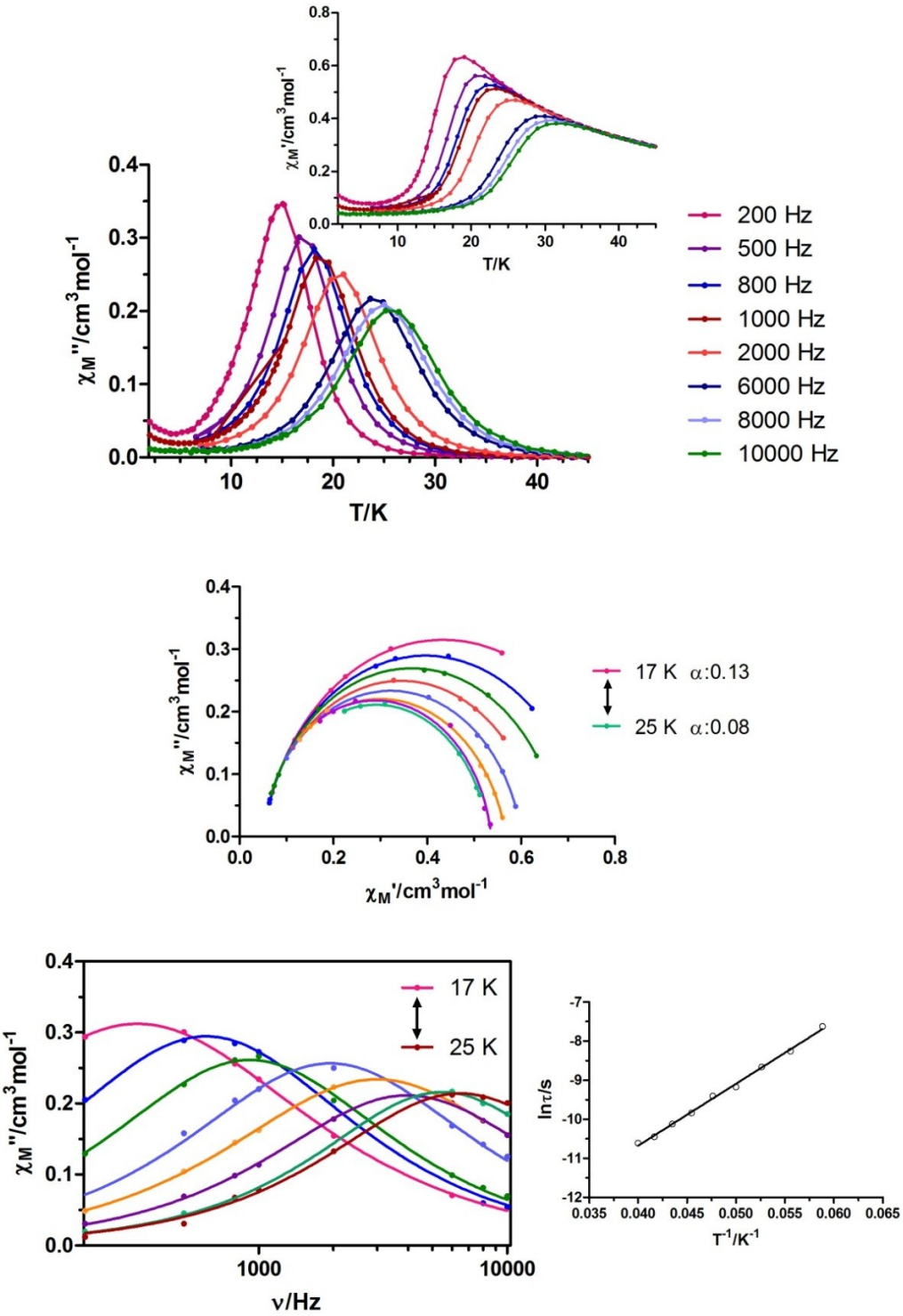

Figure S.12.- Top: temperature dependence of in-phase χ_M' (inset) and out-of phase χ_M'' components of the *alternating current* susceptibility for complex **3** under 1000 Oe applied external field. Medium: Cole-Cole plot. Bottom left: variable-temperature frequency dependence of the χ_M'' signal. Bottom right: Arrhenius plots for the relaxation of **3** (black line).

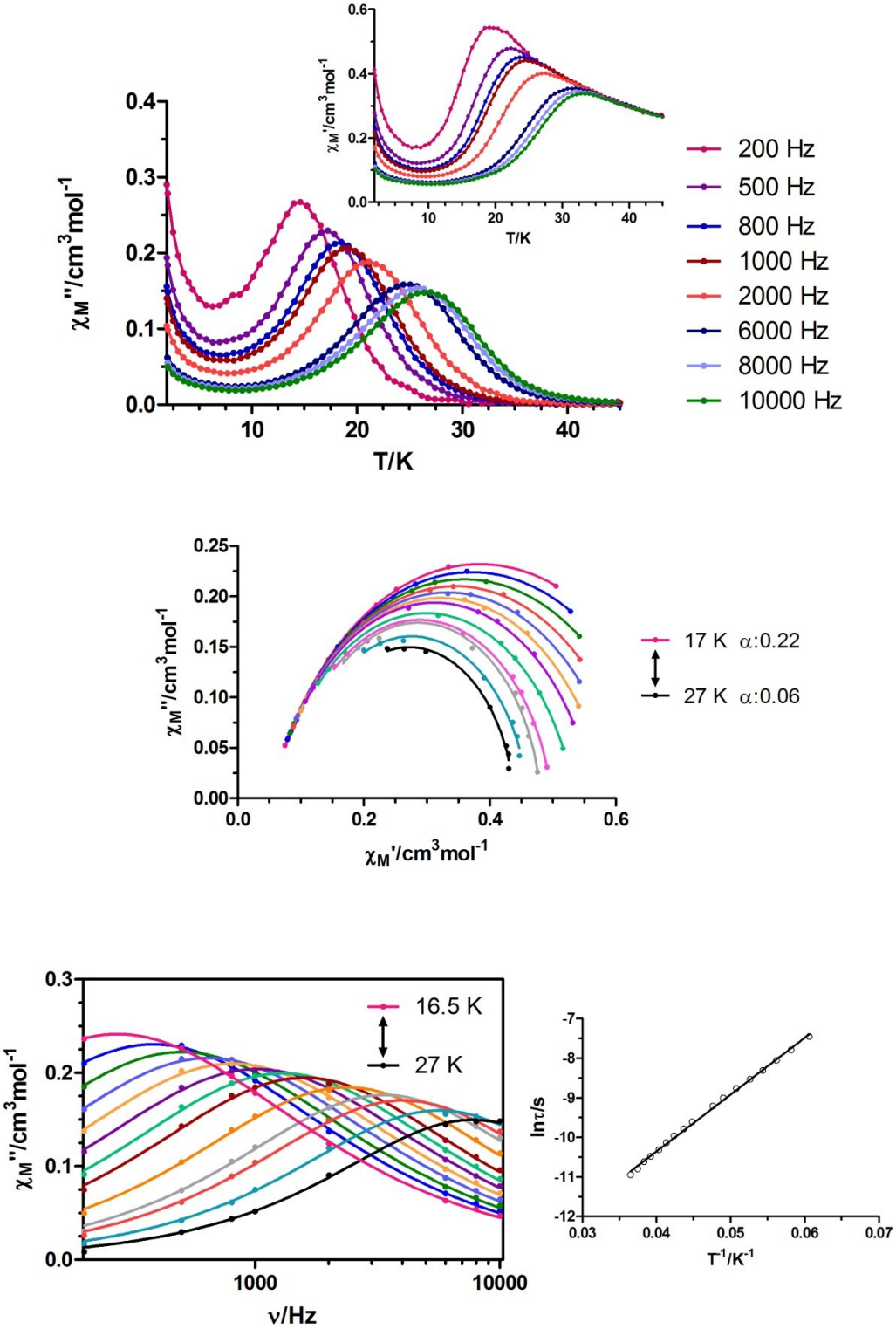

Figure S.13.- Top: temperature dependence of in-phase χ_M' (inset) and out-of phase χ_M'' components of the *alternating current* susceptibility for complex **4** under zero applied external field. Medium: Cole-Cole plot. Bottom left: variable-temperature frequency dependence of the χ_M'' signal. Bottom right: Arrhenius plots for the relaxation of **4** (black line).

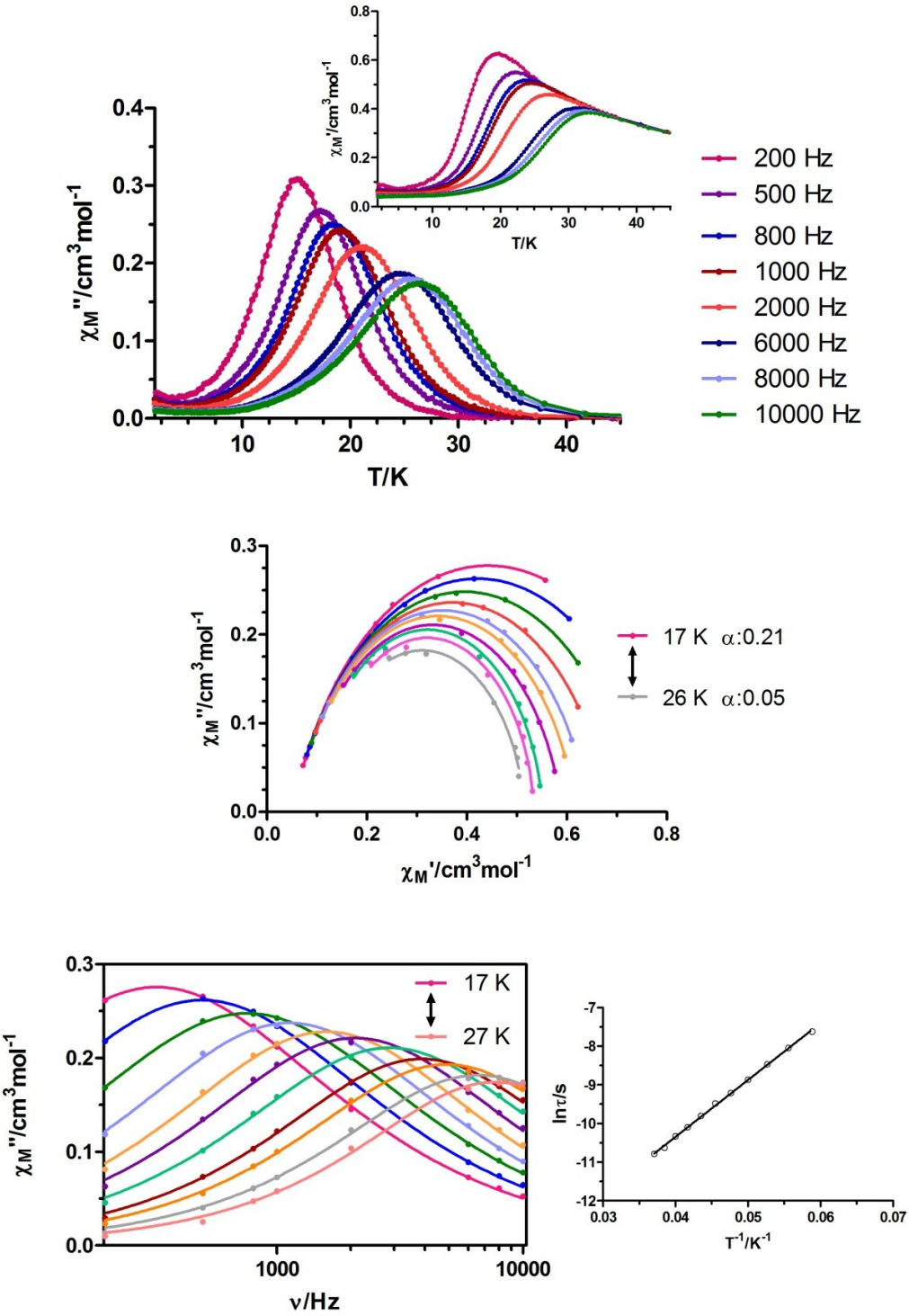

Figure S.14.- Top: temperature dependence of in-phase χ_M' (inset) and out-of phase χ_M'' components of the *alternating current* susceptibility for complex **4** under 1000 Oe applied external field. Medium: Cole-Cole plot. Bottom left: variable-temperature frequency dependence of the χ_M'' signal. Bottom right: Arrhenius plots for the relaxation of **4** (black line).

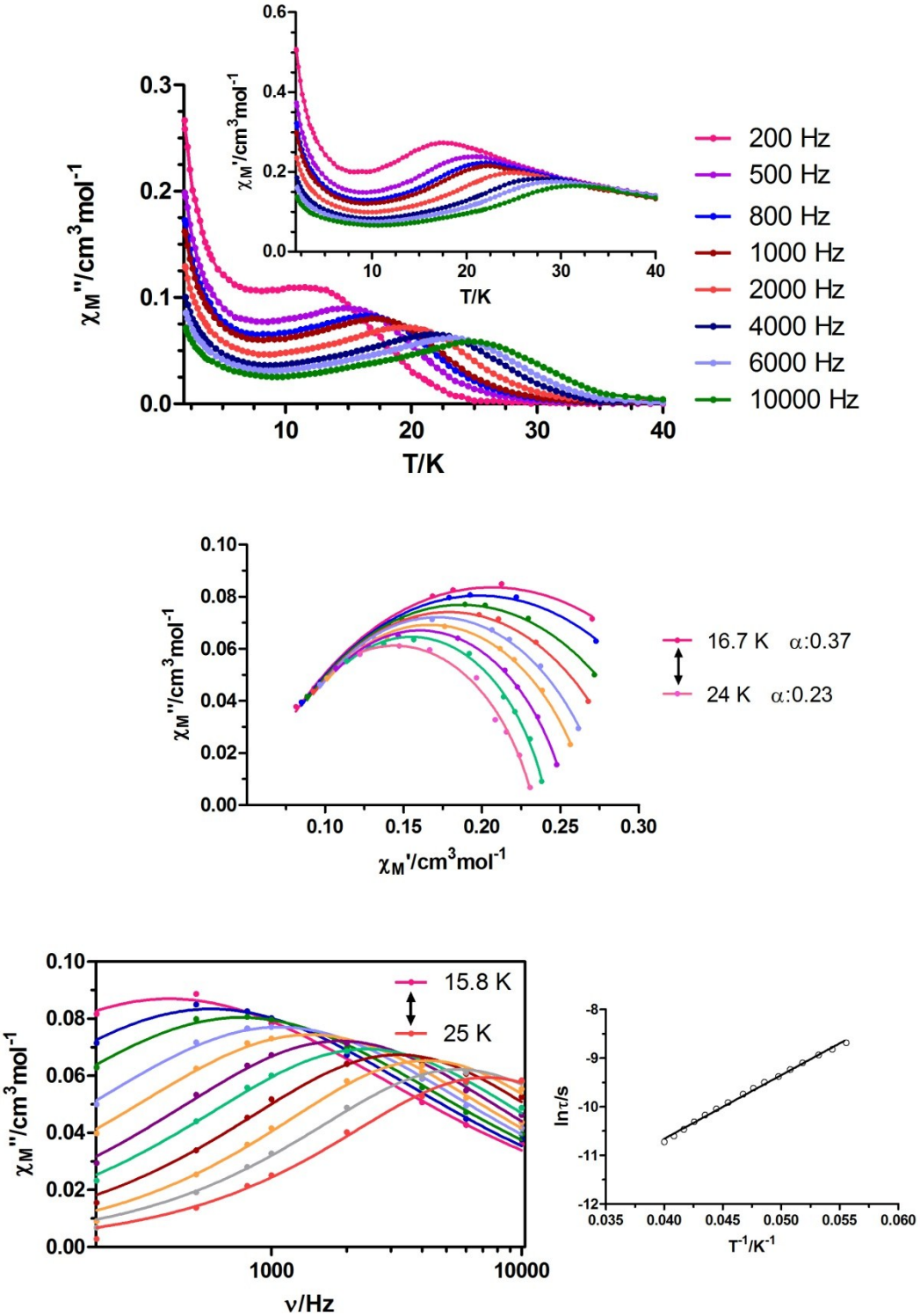

Figure S.15.- Top: temperature dependence of in-phase χ_M' (inset) and out-of phase χ_M'' components of the *alternating current* susceptibility for complex **5** under zero applied external field. Medium: Cole-Cole plot. Bottom left: variable-temperature frequency dependence of the χ_M'' signal. Bottom right: Arrhenius plots for the relaxation of **5** (black line).

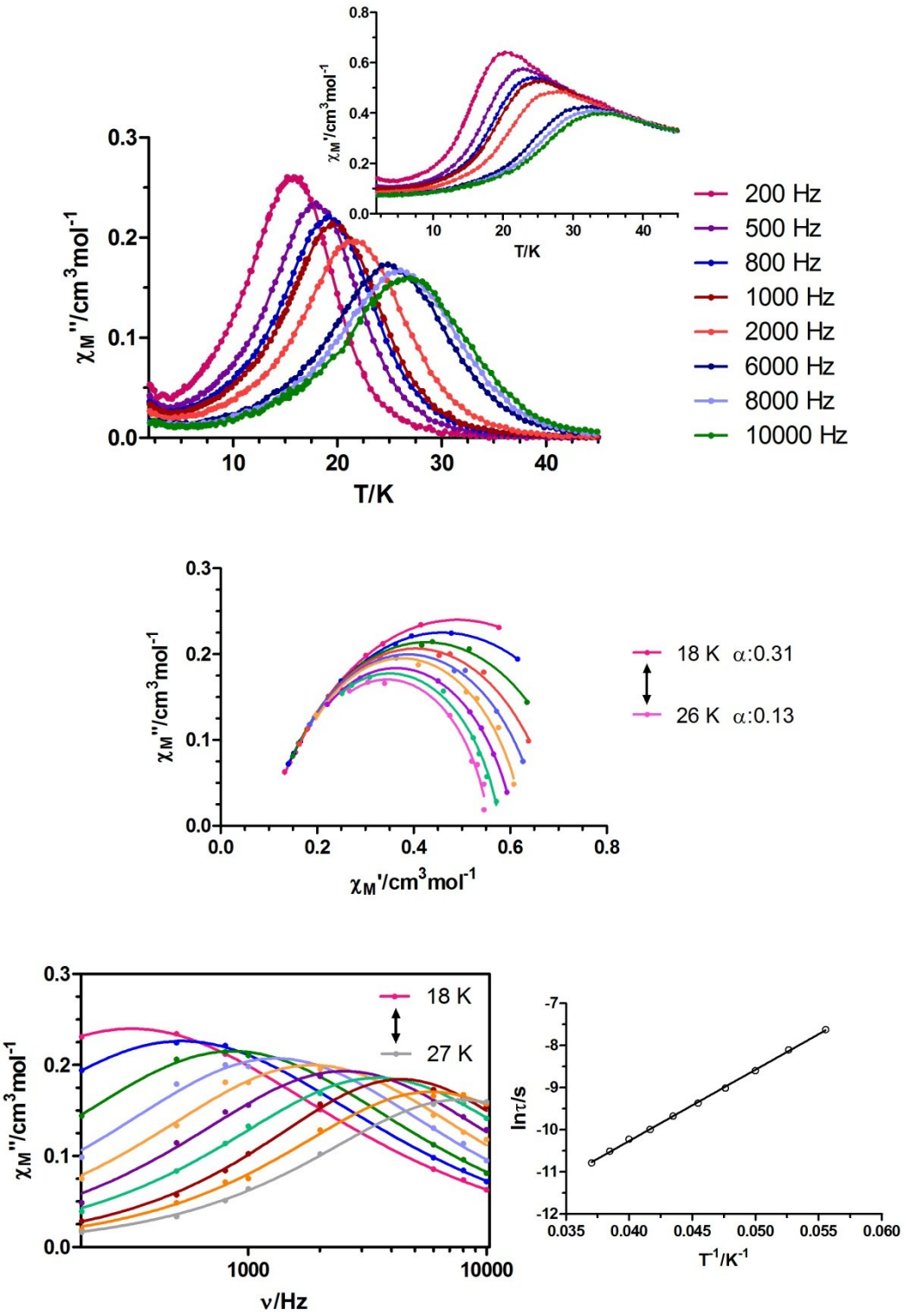

Figure S.16.- Top: temperature dependence of in-phase χ_M' (inset) and out-of phase χ_M'' components of the *alternating current* susceptibility for complex **5** under 1000 Oe applied external field. Medium: Cole-Cole plot. Bottom left: variable-temperature frequency dependence of the χ_M'' signal. Bottom right: Arrhenius plots for the relaxation of **5** (black line).

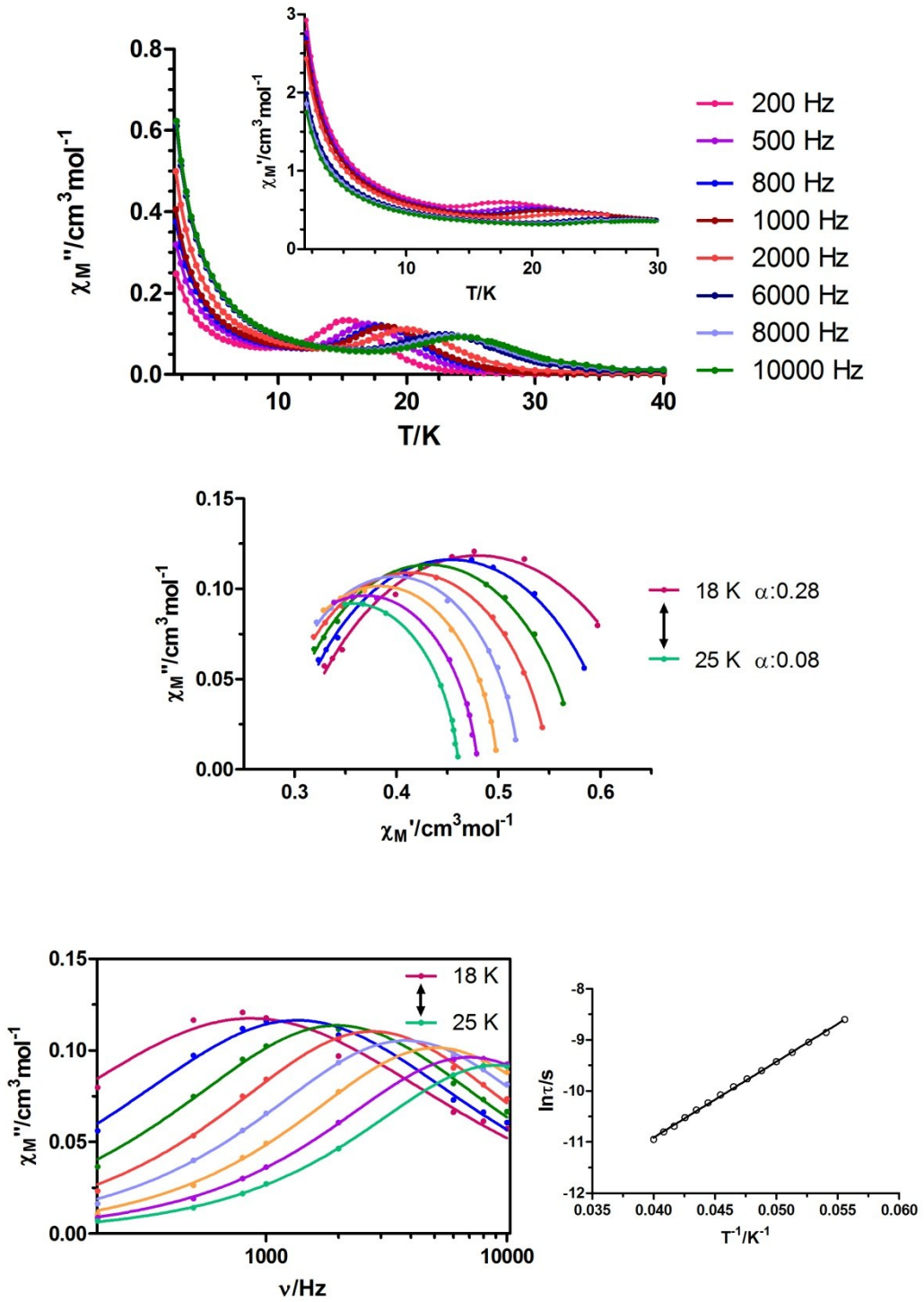

Figure S.17.- Top: temperature dependence of in-phase χ_M' (inset) and out-of phase χ_M'' components of the *alternating current* susceptibility for complex **6** under zero applied external field. Medium: Cole-Cole plot. Bottom left: variable-temperature frequency dependence of the χ_M'' signal. Bottom right: Arrhenius plots for the relaxation of **6** (black line).

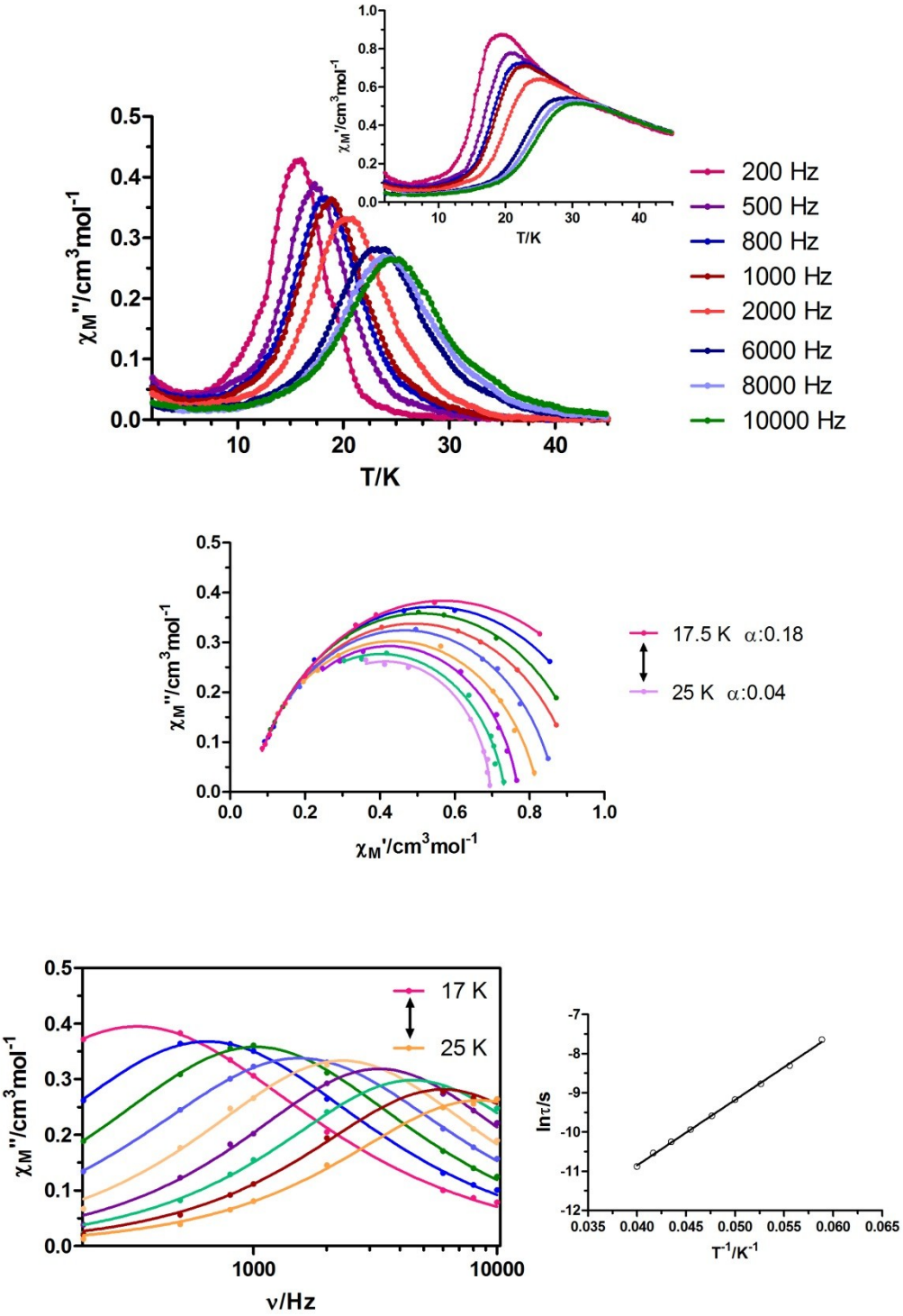

Figure S.18.- Top: temperature dependence of in-phase χ_M' (inset) and out-of phase χ_M'' components of the *alternating current* susceptibility for complex **6** under 1000 Oe applied external field. Medium: Cole-Cole plot. Bottom left: variable-temperature frequency dependence of the χ_M'' signal. Bottom right: Arrhenius plots for the relaxation of **6** (black line).

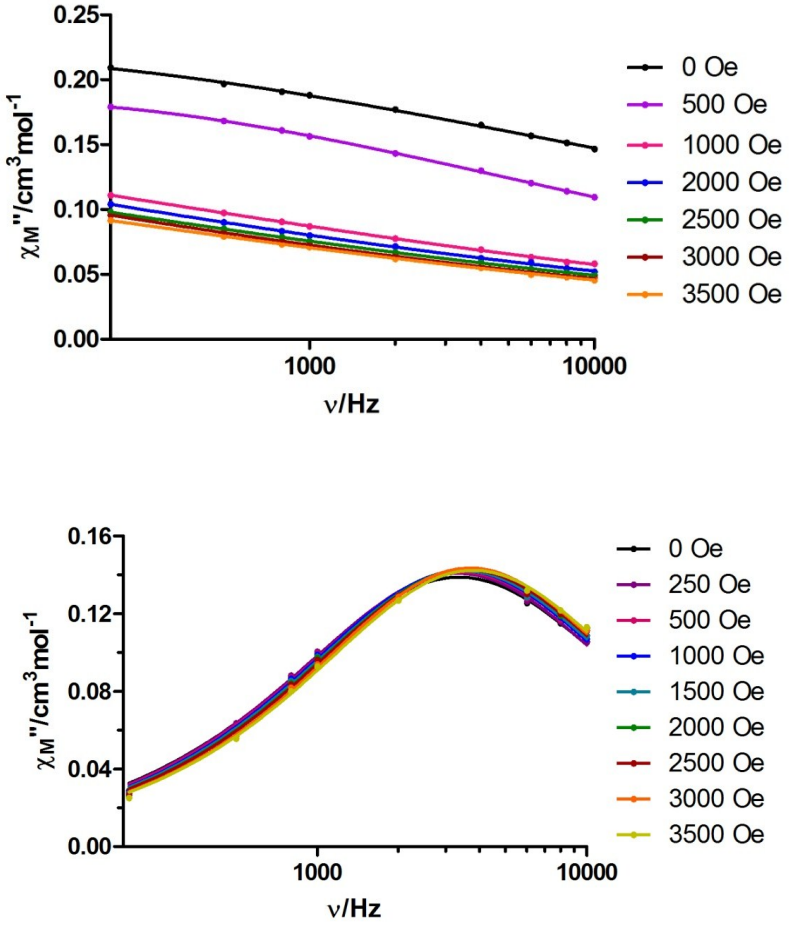

Figure S.19.- Field dependence of out-of-phase signals vs. frequency at 4 K (top) and 25 K (bottom) for **1**.

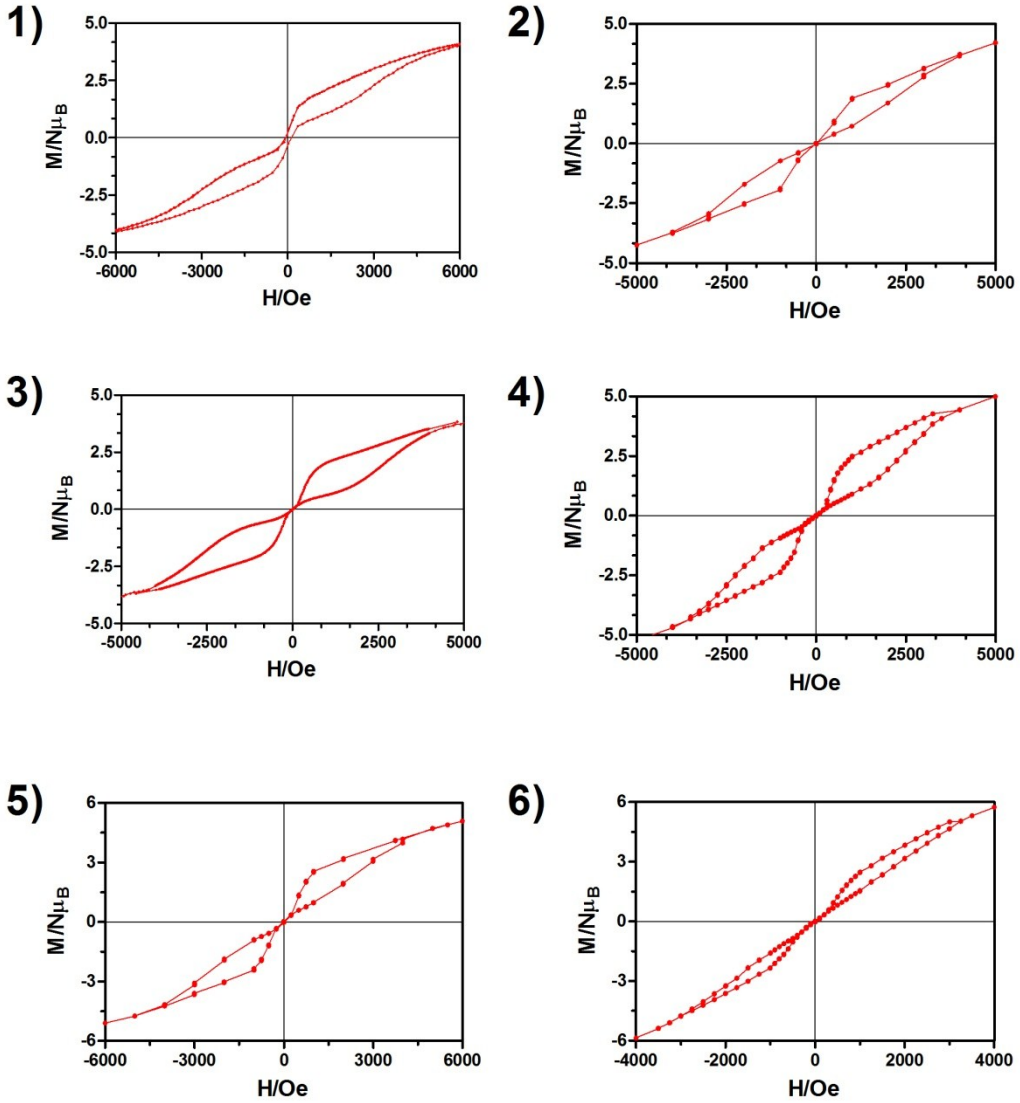

Figure S.20.- Magnetic Hysteresis loops for **1**-**6**. Red solid lines represent a guide to the eye.

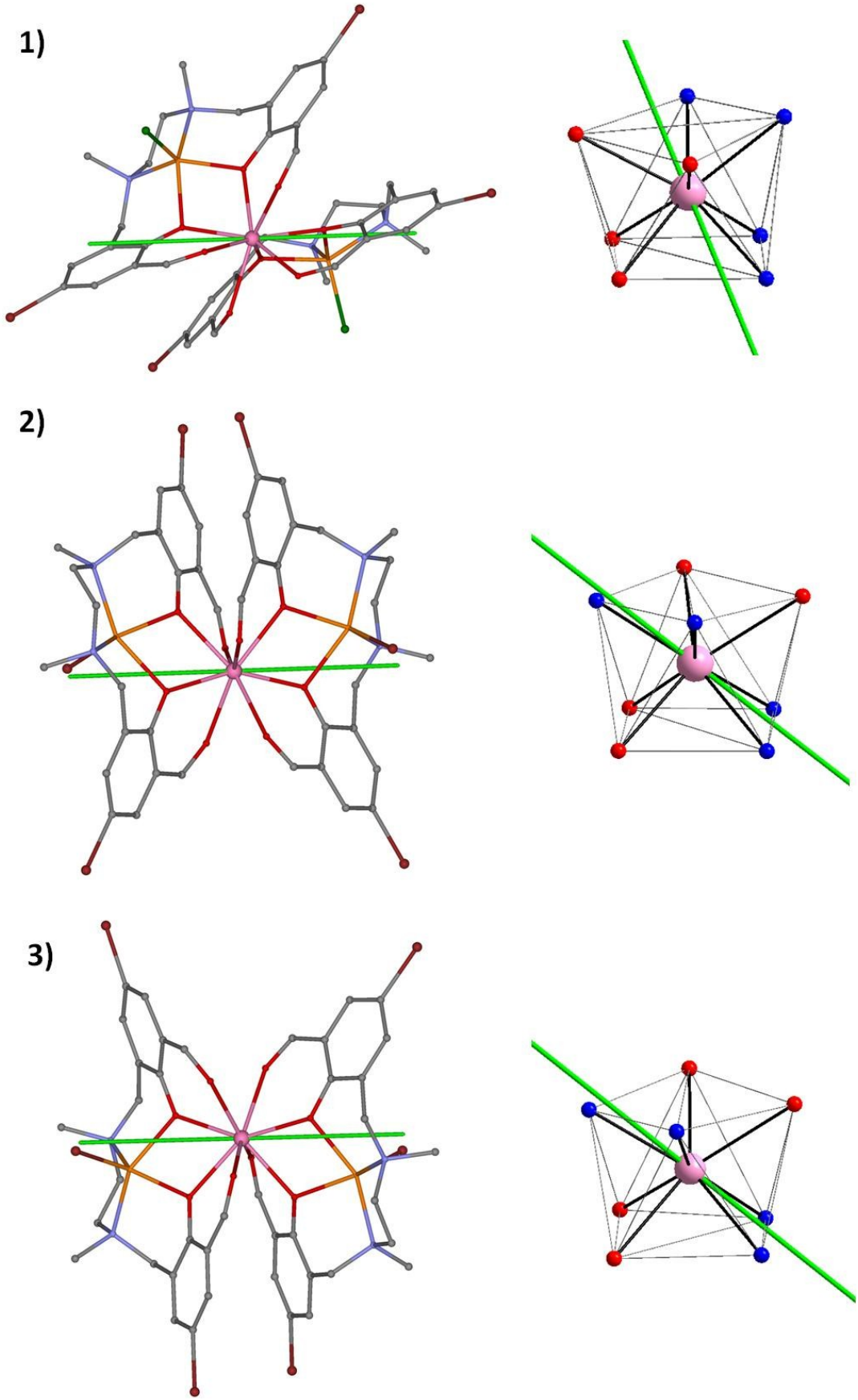

Figure S.21.- Anisotropy axis for the Dy(III) ion (green line) for **1-6** and [ZnCl(μ-L)Dy(μ-L)ClZn][$ZnCl_3(CH_3OH)$].

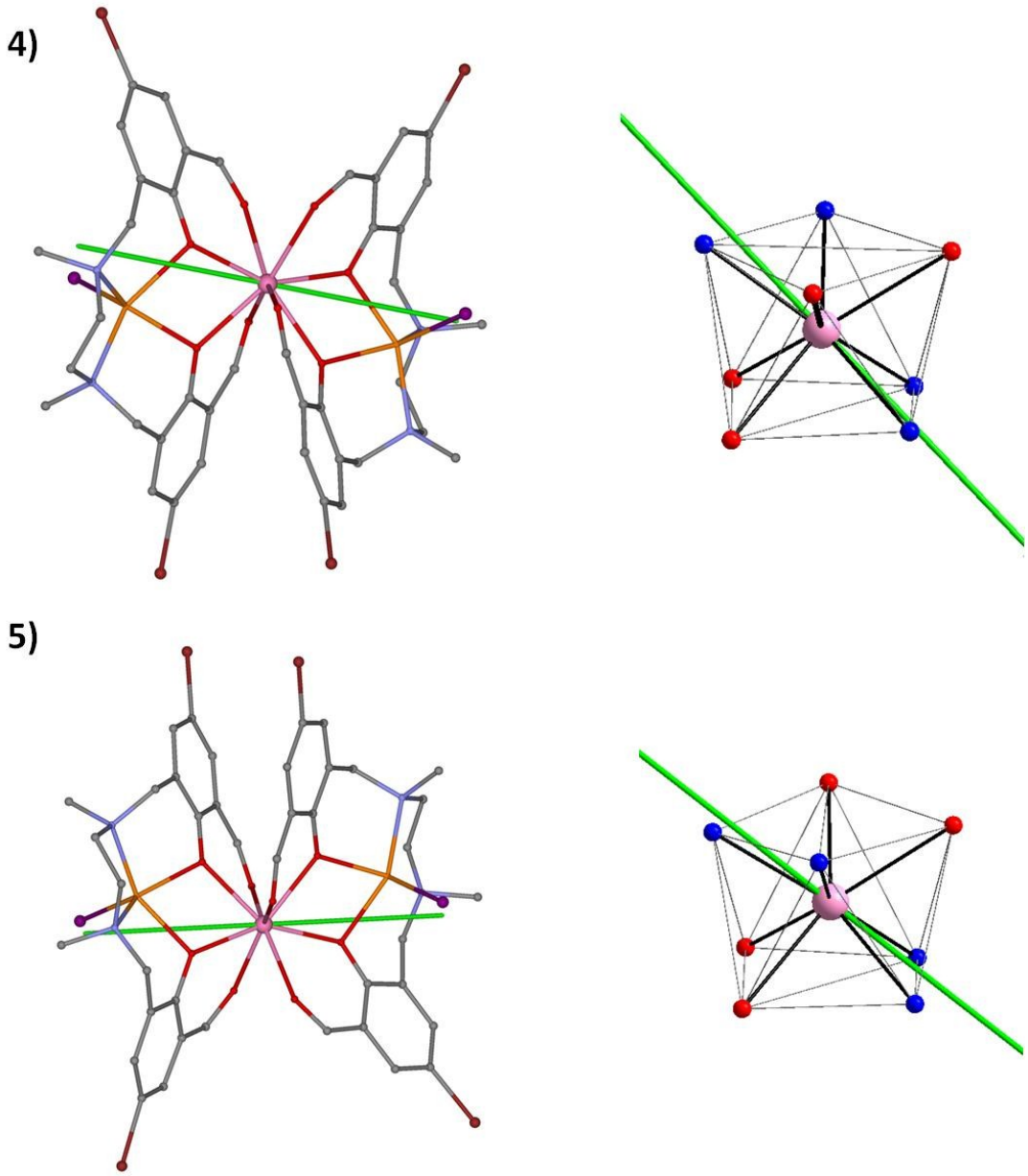

Figure S.21.- Continuation.

6)

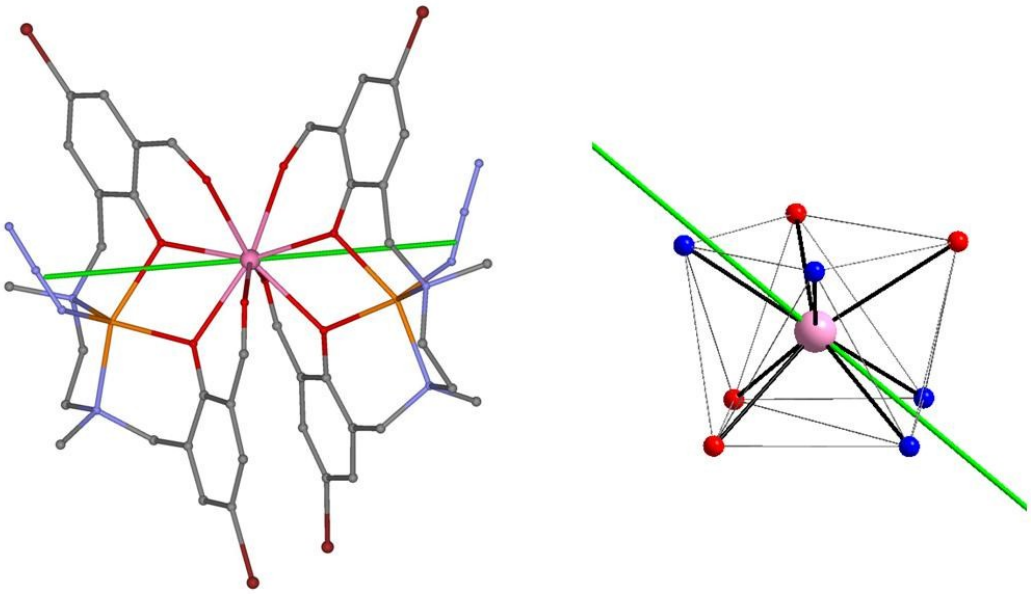

[ZnCl(μ-L)Dy(μ-L)ClZn][ZnCl$_3$(CH$_3$OH)]

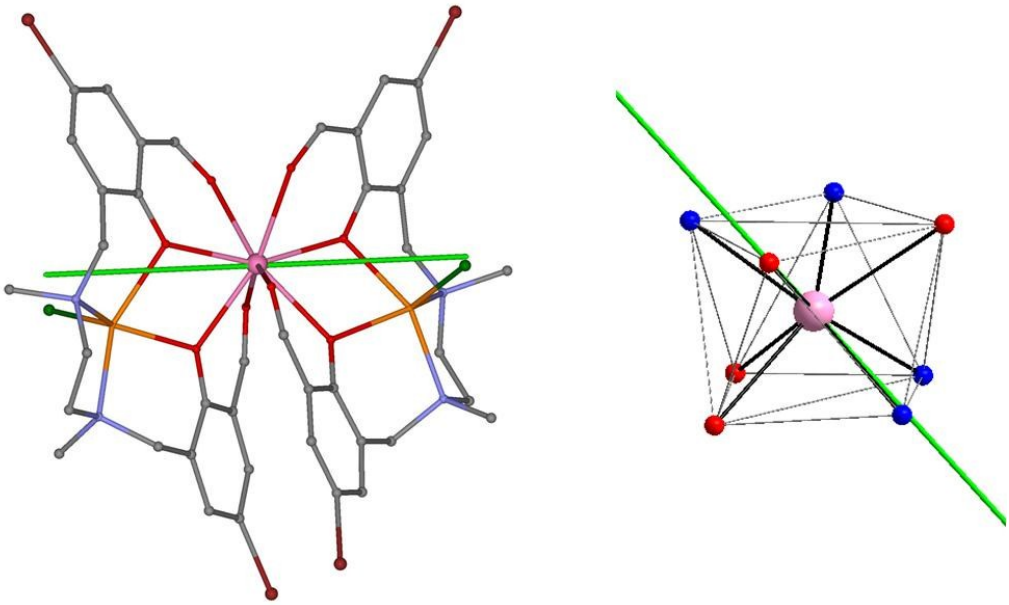

Figure S.21.- Continuation.

Table S.5- Summary of the Zn(II) and Dy(III) based SIMs.

	Complex	Closest ideal geometry by SHAPE	CshM value	U_{eff} (K)	T_B (K) Scan rate (Ts^{-1})	Ref
ZnDy	[ZnDy(**L1**)(sal)Br(NO_3)(MeOH)]	MFF-9	1.154	333 94, 336 (1000)	-	[1]
	[Zn(NO_3)(**L2**)Dy(NO_3)$_2$(H_2O)]	TCTPR-9	2.530	39.41 (900)	-	[2]
	[DyZn(**L3**)(OAc)$_2$(NO_3)]·CH_3OH	MFF-9	3.125	a (1000)	-	[3]
	[Zn(**L4**)(OAc)Dy(NO_3)$_2$]	MFF-9 (Dy1) CSAPR-9 (Dy2)	2.274 2.219	41 (1000)	b	[4]
	[Zn(**L4**)(9-An)Dy(NO_3)$_2$]·CH_3CN	MFF-9	1.668	a 32.1 (1000)	b	[4]
	[ZnDy(NO_3)$_2$(**L5**)$_2$(OAc)]	CSAPR-9	2.020	119 (3500)	-	[5]
	[ZnDy(**L6**)(DBM)$_3$]	TTD-8	2.670	a 36.5 (2000)	-	[6]
	[R,R-Zn**L7**Dy(OAc)(NO_3)$_2$]	CSAPR-9	4.762 (Dy1) 5.179 (Dy2)	19.40, 51.82 (1500)	-	[7]
	[S,S-Zn**L7**Dy(OAc)(NO_3)$_2$]	CSAPR-9	4.749 (Dy1) 5.171 (Dy2)	20.48, 51.72 (1500)	-	[7]
	[ZnDy(NO_3)$_2$(mpko)$_3$(mpkoH)]	CSAPR-9	2.348	a 33.3(1000)	-	[8]
	[ZnDy(H_2O)(phen)(mb)$_5$]	TDD-8	2.29	a 10 (1500)	-	[9]
	[(**L8**ZnBrDy(ovan)(NO_3)(H_2O)](H_2O)·0.5(MeOH)	MFF-9	0.992	119 211 (1000)	c	[10]
	[**L8**ZnClDy(thd)$_2$]	BTPR-8	1.907	99.7 160 (1000)	c	[10]
	[Zn(μ-**L**)(μ-OAc)Dy(NO_3)$_2$]·CH_3CN	CSAPR-9	1.18	a 41.55 (1000)	-	[11]
	[ZnLn(**L9H$_4$**)$_2$](NO_3)$_3$·6H_2O	SAPR-8	0.619	272	c	[12]
	[Zn(μ-**L6**)(μ-OAc)Ln(NO_3)$_2$]	CSAPR-9 MFF-9	2.196 (Dy1) 2.640 (Dy2)	27.5 (1000)	-	[13]
ZnDyZn	[Dy{Zn(**L2**)(OAc)}$_2$]BPh_4·CH_3CN	JSPC-10	1.467	6.4, 22.4 (1000)	-	[14]
	[Zn$_2$Dy(**L10**)$_2$(MeOH)]NO_3·3MeOH·H_2O	PBPY-7	0.610	439	11(0.02)	[15]
	[Zn$_2$Dy(**L10**)$_2$]NO_3·H_2O	OC-6	1.879	64 (1200)	2 (0.002)	[15]
	[Zn$_2$Dy(**L**)$_2$Cl$_2$][ZnCl$_3$(CH_3OH)]·3CH_3OH	SAPR-8	0.927	140 148 (1000)	c	[16]
	[Dy(Zn**L11**)$_2$(OAc)Cl$_2$]·CH_2Cl_2	TDD-8	2.699	a 19 (700)	-	[17]
	[ZnCl(μ-**L**)Dy(μ-**L**)ClZn]PF_6	SAPR-8	0.547	268 319 (1000)	c	[18]
	[(**L11**Zn(H_2O))$_2$Dy(H_2O)](CF_3SO_3)$_3$	MFF-9	2.582 (Dy1) 2.383 (Dy2)	139 185 (1000)	c	[19]
	[(**L11**ZnBr)$_2$Dy(H_2O)](ClO_4)	TCTPR-9	1.895 (Dy1) 2.068 (Dy2)	211 309 (1000)	c	[19]
	[(**L11**ZnCl)$_2$Dy(H_2O)](ClO_4)·1.25MeOH	TCTPR-9	1.716 (Dy1) 1.996 (Dy2)	210 291 (1000)	c	[19]
	[Zn$_2$Dy(**L12**H$_3$)$_4$]·3NO_3·2MeOH·1.5H_2O	SAPR-8	0.917	a 67 (1000)	c	[20]
	{[Dy[Zn(**L13**)Cl]$_2$(DMF)$_2$]·Cl}	SAPR-8	5.663	a (2000)	-	[21]
	[(**L14**ZnBr)$_2$Dy(MeOH)$_2$](ClO_4)	TDD-8	1.060	63.7 95.5 (1000)	c	[10]

	$[Zn_2(\mathbf{L15})_2DyCl_3]\cdot 2H_2O$	MFF-9	3.321	430[d] 481 (1000)[d]	8	[22]
	$[Zn_2(\mathbf{L15})_2Dy(MeOH)Br_3]\cdot 3H_2O$	MFF-9	2.635	233	6	[22]
	$[Zn_2(\mathbf{L15})2Dy(H_2O)Br_2]\cdot[ZnBr_4]_{0.5}$	CSAPR-9	2.115	121	4	[22]
	$[Zn_2(\mathbf{L16})_2DyCl_3]\cdot 2H_2O$	MFF-9	3.280	398[d]	8	[22]
>2Zn	$[Zn_3Dy(\mathbf{L17})(NO_3)_3(MeOH)_3]\cdot 4H_2O$	HH-9	3.726	a 25.8 (1500)	-	[23]
	$[DyZn_6(\mu_3\text{-}OH)(Gly)_6(\mu_2\text{-}NO_3)_3](OH)(NO_3)_2\cdot 8H_2O$	TCTPR-9	0.205	a 37.04 (5000)	-	[24]

[a] Maxima of the out-of-phase component of ac susceptibility is beyond the window of measurement.
[b] The T_B is below the limit of the measurement (2 K).
[c] Hysteresis loops are observed at 2 K but are not measured at higher temperatures.
[d] Values obtained taking into account the simultaneous presence of Orbach and Raman relaxation processes.

Summary of the ligands:

H_2**L1**: a Schiff-base ligand formed by a condensation reaction of o-vaniline and 2,2-dimethylpropanediamine in a 2:1 ratio. Hsal: salicylaldehyde.
H_2**L2**: N,N'-bis(3-methoxysalicylidene)-1,2-diaminoethane.
H_2**L3**: N,N′-bis(3-methoxysalicylidene)-1,2-cyclohexanediamine.
H_2**L4:** N,N′,N″-trimethyl-N,N″-bis(2-hydroxy-3-methoxy-5-methylbenzyl)diethylene-triamine. H-9-An: 9-anthracene carboxylic acid.
H**L5**: 2-methoxy-6-[(E)-phenyliminomethyl]phenol.
H_2**L6**: *N,N'*-dimethyl-*N,N'*-bis(2-hydroxy-3-methoxy-5-methylbenzyl)-ethylendiamine
HDBM: 1,3-diphenyl-propane-1,3-dione
H_2**L7**: phenol,2,2'[2,2-diphenyl-1,2-ethanediyl]bis[(E)-nitrilomethylidyne]-bis(6-methoxy).
mpkoH: methyl 2-pyridyl ketone oxime.
mb: m-methylbenzoate, phen: 1,10-phenanthroline.
H_2**L8**: N,N′-2,2-dimethylpropylenedi(3-methoxysalicylideneiminato. Ovan: ovanillin.
Thd: 2,2,6,6-tetramethyl-3,5-heptanedionato.
H_5**L9**: bi-compartmental ligand obtained by reaction of 2-formyl-6-hydroxymethyl-p-cresol with 1,3-diamino-2-propanol.
H_3**L10**: 2,2',2"-(((nitrilotris(ethane-2,1-diyl))tris(azanediyl))tris(methylene))tris-(4-bromophenol).
H_2**L11**: N,N'-2,2-dimethylpropylenedi(3-methoxysalicylideneiminato).
H_4**L12**: [2-(2-hydroxy-3-(hydroxymethyl)-5-methylbenzylideneamino)-2-methyl-propane-1,3-diol].
H_2**L13**: *N,N'*-bis(3-methoxysalicylidene)benzene-1,2-diamine.
H_2**L14**: 2-{(E)-[(3-{[(2E,3E)-3-(hydroxyimino)butan-2-ylidene]amino}-2,2-dimethylpropyl)imino]methyl}-6-methoxyphenol.
H_2**L15**: N,N'-bis(3-methoxysalicylidene)phenylene-1,2-diamine.
H_2**L16**: N,N'-bis(3-methoxysalicylidene)-1,2-diaminocyclohexane.
H_6**L17**: macrocyclic ligand.
Gly = glycine

References

[1] A. Watanabe, A. Yamashita, M. Nakano, T. Yamamura and T. Kajiwara, *Chem. Eur. J.*, 2011, **17**, 7428-7432.

[2] J. Long, R. Vallat, R. A. S. Ferreira, L. D. Carlos, F. A. A. Paz, Y. Guari and J. Larionova, *Chem. Commun.*, 2012, **48**, 9974-9976.

[3] P. Zhang, L. Zhang, S.-Y. Lin and J. Tang, *Inorg. Chem.*, 2013, **52**, 6595-6602.

[4] M. A. Palacios, S. Titos-Padilla, J. Ruiz, J. M. Herrera, S. J. A. Pope, E. K. Brechin and E. Colacio, *Inorg. Chem.*, 2014, **53**, 1465-1474.

[5] A. Upadhyay, S. K. Singh, C. Das, R. Mondol, S. K. Langley, K. S. Murray, G. Rajaraman and M. Shanmugam, *Chem. Commun.*, 2014, **50**, 8838-8841.

[6] Q.-W. Xie, S.-Q. Wu, W.-B Shi, C.-M. Liu, A.-L. Cui and H.-Z. Kou, *Dalton Trans.*, 2014, **43**, 11309-11316.

[7] J. Long, J. Rouquette, J.-M. Thibaud, R. A. S. Ferreira, L. D. Carlos, B. Donnadieu, V. Vieru, L. F. Chibotaru, L. Konczewics, J. Haines, Y. Guari and J. Larionova, *Angew. Chem. Int. Ed.*, 2015, **54**, 2236-2240.

[8] N. C. Anastasiadis, C. D. Polyzou, G. E. Kostakis, V. Bekiari, Y. Lan, S. P. Perlepes, K. F. Konidaris and A. K. Powell, *Dalton Trans.,* 2015, **44**, 19791-19795.

[9] Y. Li, C. Zhang, J.-W. Yu, E.-C. Yang and X.-J. Zhao, *Inorg. Chim. Acta,* 2016, **445**, 110-116.

[10] J. P. Costes, S. Titos-Padilla, I. Oyarzabal, T. Gupta, C. Duhayon, G. Rajaraman and E. Colacio, *Inorg. Chem.*, 2016, **55**, 4428−4440.

[11] I. Oyarzabal, B. Artetxe, A. Rodríguez-Diéguez, J. A. García, J. M. Seco and E. Colacio, *Dalton Trans.,* 2016, **45**, 9712-9726.

[12] A. Amjad, A. M. Madalan, M. Andruh, A. Caneschi and L. Sorace, *Chem. Eur. J.,* 2016, **22**, 12849-12858.

[13] A. Zabala, J. Cepeda, I. Oyarzabal, A. Rodriguez-Dieguez, J. A. Garcia, J. M. Seco and E. Colacio, *CrystEngComm*, 2017, **19**, 256-264..

[14] M. Maeda, S. Hino, K. Yamashita, Y. Kataoka, M. Nakano, T. Yamamura and T. Kajiwara, *Dalton Trans.*, 2012, **41**, 13640-13648.

[15] J.-L. Liu, Y.-C. Chen, Y.-Z. Zheng, W.-Q. Lin, L. Ungur, W. Wernsdorfer, L. F. Chibotaru and M.-L. Tong, *Chem. Sci.,* 2013, **4**, 3310-3316.

[16] I. Oyarzabal, J. Ruiz, J. M. Seco, M. Evangelisti, A. Camón, E. Ruiz, D. Aravena and E. Colacio, *Chem. Eur. J.,* 2014, **20**, 14262-14269.

[17] P.-Y. Shan, H.-F. Li, P. Chen, Y.-M. Tian, W.-B. Sun and P.-F. Yan, *Z. Anorg. Allg. Chem.*, 2015, **641**, 1119-1124.

[18] I. Oyarzabal, J. Ruiz, E. Ruiz, D. Aravena, J. M. Seco and E. Colacio, *Chem.*

Commun., 2015, **51**, 12353-12356.

[19] J. P. Costes, S. Titos-Padilla, I. Oyarzabal, T. Gupta, C. Duhayon, G. Rajaraman and E. Colacio, *Chem. Eur. J.,* 2014, **20**, 14262-14269.

[20] S. Das, K. S. Bejoymohandas, A. Dey, S. Biswas, M. L. P. Reddy, R. Morales, E. Ruiz, S. Titos-Padilla, E. Colacio and V. Chandrasekhar, *Chem. Eur. J.,* 2015*,* **21**, 6449-6464.

[21] Q. Ma, S. Zeng, X. Feng, W. Cao, H. Wang, J. Dou and J. Jiang, *Eur. J. Inorg. Chem*., 2016, 4194-4198.

[22] W.-B. Sun, P.-F. Yan, S.-D. Jiang, B.-W. Wang, Y.-Q. Zhang, H.-F. Li, P. Chen, Z.-M. Wanga, S. Gao, *Chem. Sci*., 2016, **7**, 684-691.

[23] H. L. C. Feltham, Y. Lan, F. Klöwer, L. Ungur, L. F. Chibotaru, A. K. Powell, S. Brooker, *Chem. Eur. J*., 2011, **17**, 4362-4365.

[24] G. Xiong, X.-Y. Qin, P.-F. Shi, Y.-L. Hou, J.-Z. Cui, B. Zhao, *Chem. Commun*., 2014, **50**, 4255-4257.